Wireless Channel Characterisation in Burning Buildings over 100–1000 MHz

Andrew C. M. Austin, *Member, IEEE*

***Abstract*—A three-dimensional implementation of the finite-difference time-domain (FDTD) method is used to model 100–1000 MHz radiowave propagation in a generalised office building. Fire within this building is modelled as a cold plasma medium. The presence of fire is found to decrease the sector-averaged received power by up to 10 dB. The FDTD results also show propagation through fire can introduce rotation in linearly polarised signals, increasing the power of cross-polarised components. Uncertainties in the plasma properties are modelled using non-intrusive polynomial chaos, and can introduce up to ± 8 dB variation in the sector-averaged power.**

***Index Terms*—Indoor propagation, Fires, Finite difference methods.**

I. Introduction

Building fires are devastating events that can cause significant damage to property and, more importantly, threaten human life. Firefighters often need to enter burning buildings to extinguish fires and rescue people who may be trapped. To communicate with each other and with fire crews coordinating the efforts outside the building, firefighters are usually equipped with radios operating in the VHF and lower UHF frequency bands (for example, the New Zealand Fire Service uses 450–500 MHz within cities and urban environments, and 140 MHz systems in rural areas [1]). At these frequencies, good coverage can usually be achieved within buildings, as the radio waves will typically propagate through the internal and external walls [2, pp. 196–197]. However, in burning buildings, the presence of fire (with sufficient energy) will cause the formation of plasma [3], [4], [5]. In a plasma medium, free electrons and ions can interact with radio waves, significantly altering the propagation paths and mechanisms, potentially reducing the performance and reliability of the wireless communication systems used by firefighters.

Previous research has examined the impact of fire on outdoor and terrestrial radio systems analytically, using Kirchoff integration [6]; via experimental measurements [3], [7]; and though numerical methods, such as the FDTD [4]. The experimental results reported in [7] measured RF propagation through three large bonfires (consisting of timber and other plant matter) and were conducted outdoors. The temperature of these fires was estimated to be 1300–1600 K [7]. In all cases, significant attenuation (up to 15 dB for a 7.0 m diameter fire) was observed immediately after the fire ignition, particularly around 400 MHz [7]. Similarly, [5] reported 1.6–5.8 dB attenuation of the line-of-sight (LOS) signal for a controlled fire (fuelled with pine wood, reaching a maximum temperature of 1000 K) with a 0.5 m diameter over the 8–10.5 GHz frequency range. At lower frequencies (50–1000 MHz), other outdoor experiments demonstrated propagation through large hydrocarbon-fuelled fires also introduced rotation of polarised signals [3]. Modelling the fire as a plasma medium has been shown to accurately predict the experimental observations, particularly the attenuation experienced when the fire occludes the LOS path [5], [4], [8]. However, the properties of the fire-induced plasma medium depend on the fire dynamics and the fuel, both of which can have associated uncertainties [8, pp. 60–65].

Contributions: This paper investigates the impact of fire on the indoor wireless channel over the upper VHF and lower UHF frequency bands. It should be noted that the analysis of radio propagation through burning buildings has not been previously reported in the literature. Results for propagation through fire in (largely open) outdoor environments may not be directly applicable to indoor environments, where the internal building structure can also significantly influence the propagating signals, e.g., via reflection and diffraction [9]. The difficulties and dangers of conducting experimental measurements inside burning buildings motivates a numerical investigation. To capture the complex interactions with the fire-induced plasma medium, a three-dimensional implementation of the FDTD method is used to model the 100–1000 MHz radio channel for a typical office building. Fire within the building is modelled using a cold plasma model [5], [8], and the impact of uncertainty in the electrical properties of the plasma on the FDTD simulation results is analysed using the polynomial chaos method.

II. Modelling Propagation through Fire

Flames induce a partial thermal ionisation of the gaseous components surrounding a fire [10], [3]. This phenomena is termed a cold plasma (cold here refers to the partial ionisation and not the temperature). An electromagnetic field impinging on a partially ionised gas displaces free electrons from their mean position, thereby inducing a polarisation current $\mathbf{J_p}$, given by

$$\frac{\partial \mathbf{J_p}}{\partial t} = -\nu \mathbf{J_p} + \epsilon_0 \omega_p^2 \mathbf{E} \tag{1}$$

where ν is the collision frequency (in Hz), ω_p is the plasma frequency (in rad/s), and $\mathbf{E}$ is the vector electric field. The plasma frequency is given by

$$\omega_p = \sqrt{\frac{N_e e^2}{\epsilon_0 m}} \tag{2}$$

where e and m are the electron charge and mass respectively, and N_e is the electron density (m^{-3}). The collision frequency and electron density depend on the relative concentration (and types) of ions in the plasma and on the surrounding temperature and pressure. The nominal values for the plasma properties used in this paper are based on reported measurements of ν and N_e from a pine wood fire: $\nu \approx 10^{10}$–10^{11} Hz and $f_p \approx 850$ MHz [5]. While timber made from pine wood is widely used in buildings as framing for internal walls and partitions, many other flammable materials (with different plasma properties) are often present in varying and unknown quantities. The impact of this resulting uncertainty in the plasma properties is considered in section IV.

A.C.M. Austin is with the Telecommunication Circuits Laboratory, Ecole Polytechnique Federale de Lausanne (EPFL), Lausanne 1015, Switzerland, e-mail: acm.austin@ieee.org

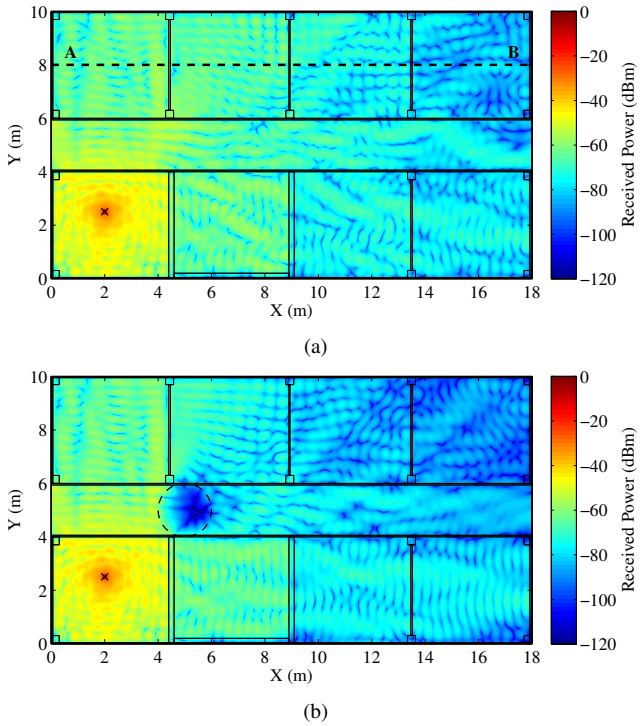

Fig. 1. Power recorded on a slice positioned 1.3 m above the floor at 450 MHz (a) without fire and (b) 1 m radius fire, contained within the dashed locus (- - -) with $f_p = 850$ MHz and $\nu = 10^{10}$ Hz.

The polarisation current is included in Maxwell's equations as an additional current source. The frequency-dependent behaviour of the plasma medium can then incorporated into the FDTD algorithm via auxiliary update equations for (1), and by including the polarisation current in the update equations for the electric field components [11, pp. 361–368][8, pp. 96–98].

III. FDTD Simulation Results

The floor plan for the indoor environment considered is shown in Fig. 1(a). The dimensions are 18 m $\times$ 10 m $\times$ 3 m and the volume is discretised using a 2 cm rectangular mesh, resulting in approximately 84×10^6 mesh cells when the 12-cell thick convolutional perfectly-matched layer surrounding the working volume is included. The FDTD lattice is excited with a modulated Gaussian pulse—with centre frequency 500 MHz, and 200 MHz 3 dB bandwidth—and run for 4000 time-steps. On a 2.3 GHz Intel i7 processor each simulation requires approximately 6.6 GB of memory and takes two hours to complete. The position of the transmitting antenna, assumed to be a vertically-orientated short dipole, is indicated by $\times$ and located 1.3 m above the floor. The building geometry consists of a 0.2 m thick concrete floor and ceiling ($\epsilon_r = 4.0$ and $\sigma = 50.0$ mS/m) and 6 cm thick drywall ($\epsilon_r = 3.0$ and $\sigma = 2.0$ mS/m) internal partitions. Two internal partitions are assumed to be made from concrete to act as structural supports, along with concrete pillars placed along the corridor and the building exterior. The exterior walls are assumed to be glass with $\epsilon_r = 3.0$ and $\sigma = 2$ mS/m.

Fig. 1(a) shows the steady-state power (in dBm) of the E_z component recorded at 450 MHz across the floor of the building (on a slice 1.3 m above the floor) when the fire is not present. Local variations in the received power are visible and are caused by multi-path fading. On a larger scale, the internal structure of the building constrain and guide the radio waves, leading to lower power in regions of the building that are shadowed by the internal walls. As shown in Fig. 1(b), the presence of fire in the corridor—which is modelled as a 1 m radius (discretised) sphere of cold plasma medium and contained within the dashed region—significantly reduces the power received in many regions of the building. For the results shown in Fig. 1(b), the nominal fire properties are: $f_p = 850$ MHz and $\nu = 10^{10}$ Hz. Similar results are observed when the fire parameters are changed over the range given in Table I, and the impact of uncertainty is further analysed in the following section. Up to 100 dB attenuation is observed within the fire as the operating frequency is on the same order of magnitude as the plasma frequency. The fire thus casts a significant radio shadow and blocks the dominant propagation paths, leading to significantly decreased power across the floor.

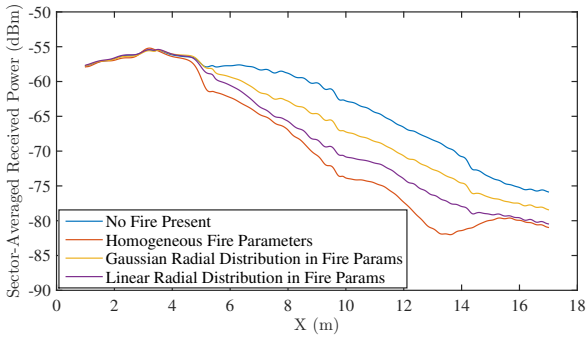

Fig. 2. Sector-averaged received power (E_z component at 450 MHz) along line **AB** for various radial distributions of the fire parameters.

In Fig. 1(b) the fire is modelled as a sphere of homogenous plasma, i.e., with constant intensity. In reality, the fire intensity would tend to be distributed, with higher temperatures in the centre of the fire potentially resulting in increased plasma effects. Accordingly, the variation in the fire intensity has been modelled by introducing Gaussian and linear radial distributions for ν and f_p though the plasma sphere. For both, the maximum value is attained in the centre of the plasma sphere, while the minimum is placed on the outside surface. Fig. 2 shows the sector-averaged received power along line **AB** for the cases when no fire is present, and with homogeneous, linear- and Gaussian-distributed plasma parameters. Multi-path fading is removed by spatially averaging the received power over a $2\lambda \times 2\lambda$ region [12]. When the fire is assumed to have a constant intensity, the sector-averaged power is reduced by up to 11 dB. As expected, the power decreases significantly when moving into regions shadowed by the fire (i.e., $x > 6$ m). Considerable spatial variation is also observed, as the fire attenuates the LOS path so that other more complex propagation mechanisms dominate, e.g., diffraction from the concrete pillars, or reflection from the windows and walls. Fig. 2 also shows that when ν and f_p are Gaussian- and linearly-distributed through the sphere, the received power is

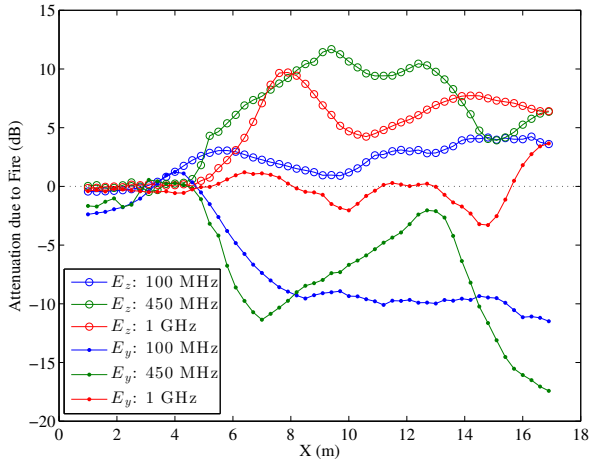

Fig. 3. Attenuation in the sector-averaged power, introduced by the fire, along the line **AB** for E_y and E_z field components at 100, 450 and 1000 MHz.

decreased by up to 5 dB and 8 dB respectively. These results suggest that while the internal composition of the plasma can impact the propagation across the floor, a homogeneous model captures the dominant effects.

Fig. 3 shows the relative attenuation (calculated as the sector-averaged field ratio relative to the case without the fire present) along the line **AB** for the linearly polarised E_z field component and the cross-polarised E_y component at 100, 450 and 1000 MHz. The fire is assumed to have homogenous plasma parameters. The attenuation is lowest at 100 MHz, and generally increases with frequency. It is also observed that the E_y field components in regions shadowed by the fire have a negative attenuation, i.e., a relative gain. In particular, the gain on the E_y component is relatively constant and approximately 10 dB at 100 MHz; while at 1 GHz, the gain is lower and bounded within ± 4 dB. Fig. 3 shows the linearly polarised E_z components are attenuated by interactions with the plasma medium, while the strength of the cross-polarised E_y component are increased, and though not shown for clarity, a similar increase is also observed for the E_x component. A possible explanation for this observation is Faraday rotation, whereby linearly polarised signals travelling through a plasma medium are rotated [13, pp. 144–145]. Furthermore, previous experimental measurements of LOS propagation through a fire have reported significant rotation of both vertically and horizontally polarised signals over 100–1000 MHz [3].

IV. Uncertainties in the Fire-induced Plasma

The uncertainty in the chemical composition of the fuel (construction materials, furniture and other flammable objects) present in the building will introduce uncertainty in the fire dynamics—e.g., the temperature and pressure—and in the electrical properties, ω_p and ν, of the fire-induced plasma. Furthermore, these parameters will also change over time and space as the fire progresses. Hence, ω_p and ν are considered random variables and are characterised with appropriate probability density functions (PDFs), as shown in Table I.

TABLE I
Fire parameters and associated uncertainty

	Nominal Value	Distribution	Uncertainty (3σ range)
Collision freq., ν	10^{10} Hz	Log-Normal	6.3×10^9 – 1.6×10^{11}
Plasma freq., f_p	850 MHz	Gaussian	450 MHz – 1.3 GHz

The uncertainty about the nominal values is estimated from experimental measurements: $\nu = 3.4$–6.0×10^{10} Hz and $N_e = 0.5$–1.4×10^{16} m^{-3} [5]. However, thermal ionisation models of combustion induced plasma [8, pp. 60–65] and theoretical analyses of atmospheric cold plasma media [14], generally predict a wider range of values for ν, ranging from 3×10^9–4×10^{11} Hz. Accordingly, in this analysis the uncertainty in ν is increased and assumed to be log-normally distributed.

A. Polynomial Chaos Expansion

The uncertainty in ω_p and ν will introduce randomness in the FDTD simulation results, which cannot be analysed using a single simulation run (at the nominal values or otherwise). However, for indoor channel considered in this paper, the Monte Carlo method is inappropriate, given the slow convergence of Monte Carlo methods (typically proportional to $\frac{1}{\sqrt{N}}$, where N is the number of trials) and the computational resources required for each FDTD simulation. Previous research has shown non-intrusive polynomial chaos techniques can accurately estimate uncertainty in FDTD models of the indoor radio channel (arising from randomness in the dielectric properties and geometry), and are substantially less computationally expensive than Monte Carlo based methods [15].

The polynomial chaos method is used to construct a surrogate model, R', for the FDTD simulation results, R, (the sector-averaged received power at any point in space) in terms of the N uncertain input parameters. In particular, R' is approximated by a weighted summation of orthogonal basis polynomials in the random input parameter space. As we have two uncertain variables, ν and ω_p,

$$R(\nu, \omega_p) \approx R'(\nu, \omega_p) = \sum_{j=0}^{P} a_j \psi_j(\nu) \phi_j(\omega_p) \qquad (3)$$

where a_j is the weighting coefficient and $\phi_j(\omega_p)$ and $\psi_j(\nu)$ are the polynomial chaos basis functions. The number of terms, P, is given by $\frac{(N+D)!}{N!D!}$, where D is the highest polynomial order. As ω_p follows a Gaussian probability distribution, $\phi_j(\omega_p)$ is a Hermite polynomial (in accordance with the Askey scheme [16]). However, as ν follows a log-normal distribution, we define $\rho = \log_{10} \nu$ and write the expansion in terms of ρ, thus allowing Hermite polynomials to be used to expand both uncertain variables. The weighting coefficients can be found

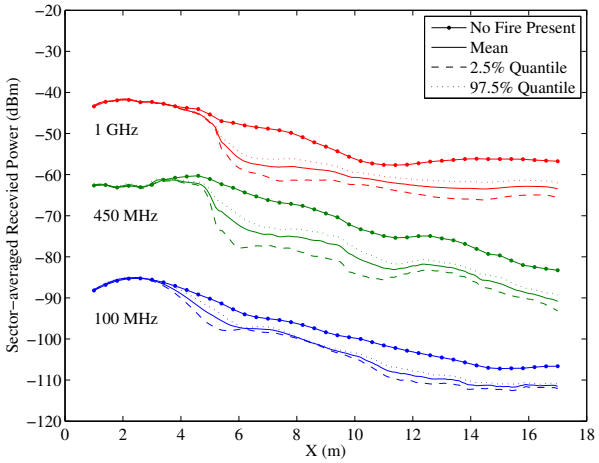

Fig. 4. Uncertainty in the power recorded along the line **AB** due to randomness in the electrical properties of the fire at 100, 450 and 1000 MHz.

via projection,

$$a_j = \frac{\left\langle R(\rho,\omega_p), \phi_j(\rho)\phi_j(\omega_p) \right\rangle}{\left\langle \phi_j^2(\rho)\phi_j^2(\omega_p) \right\rangle} = \frac{1}{\left\langle \phi_j^2(\rho)\phi_j^2(\omega_p) \right\rangle} \iint R(\rho,\omega_p)\, \phi_j(\rho)\phi_j(\omega_p)\, d\rho\, d\omega_p \quad (4)$$

where the integration is over the input parameter space. The multi-dimensional integral in (4) can be evaluated using numerical quadrature, e.g.

$$\iint R(\rho,\omega_p)\, \phi_j(\rho)\phi_j(\omega_p)\, d\rho\, d\omega_p \approx \sum_q R\left(\rho^{\{q\}}, \omega_p^{\{q\}}\right) \phi_j^{\{q\}}(\rho)\phi_j^{\{q\}}(\omega_p) w^{\{q\}} \quad (5)$$

where $\rho^{\{q\}}$ and $\omega_p^{\{q\}}$ are the quadrature points and $w^{\{q\}}$ are the weights. Thus to construct the surrogate model, the full FDTD simulation needs to be run for the set of $\{q\}$ input parameters, corresponding to the quadrature points in (5).

B. Results and Discussion

Fig. 4 shows the variation in the sector-averaged power along **AB**, when the plasma properties are assumed to follow the distributions outlined in Table I (the size of the fire and its position in the indoor environment are held constant). Also shown is the power recorded on **AB** without the fire present, which tends to decrease with x due to increasing separation from the transmitting antenna. The uncertainty due to randomness in ν and ω_p is quantified by expanding the uncertain fields using (3), with maximum order $D = 2$. Using Kronrod-Patterson quadrature, a total of nine simulations were required to estimate the coefficients in (5). The mean and 95% confidence intervals are computed directly from the polynomial chaos surrogate model.

Randomness in the fire parameters will introduce varying levels of attenuation for the LOS signal, and will alter the magnitude and phase of components reflected, diffracted and scattered from the fire surface. Accordingly, in regions where the strong LOS path is not blocked by the fire (i.e $x < 5$ m), the uncertainty in ν and ω_p typically has little impact, and the 95% confidence interval for the sector-averaged power is bounded between ± 1 dB of the mean value. In contrast, moving into regions where the LOS propagation path is occluded ($x > 5$ m) results in a greater variation. It is observed that the lowest variation occurs at 100 MHz, and the size of the 95% confidence intervals generally increase with frequency (over 100–1000 MHz). This occurs as the mean plasma frequency is 850 MHz, and thus variations in the fire parameters will have greatest impact on transmissions with operating frequencies around that value. It is noted that while the input uncertainties are relatively large, the predicted spread (measured using the 95% confidence interval) in the sector-averaged power is bounded within ± 8 dB of the mean value for all sectors considered. For example, Fig. 5 shows the probability distribution of the 450 MHz sector-average power at $X = 6$ m. The distribution is skewed, so that while 95% of the power is expected to lie between -78 dBm and -70 dBm, values below -80 dBm are possible, albeit with low probability.

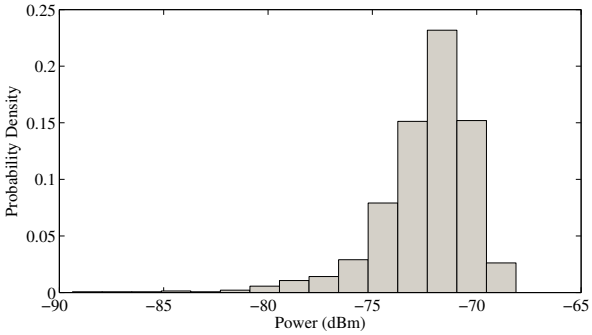

Fig. 5. Variation in the $2\lambda \times 2\lambda$ sector-averaged power at 450 MHz (centred at $x = 6$ m, $y = 8$ m) due to uncertainty in the plasma properties given in Table I.

V. Conclusion

The impact of fire (modelled as a cold plasma medium) on the 100–1000 MHz indoor wireless channel has been analysed using a three-dimensional implementation of the FDTD method. The FDTD simulation results show fire-induced plasma can introduce strong local attenuation, thereby altering propagation mechanisms and paths. Propagation through fire was also found to rotate linearly polarised signals, significantly increasing the power of cross-polarised components, relative to case without the fire present. The uncertainties in the simulated results (due to randomness in the plasma properties) were efficiently computed using polynomial chaos expansions, and are within ± 8 dB of the mean values.

References

[1] "Register of radio frequencies," accessed April 2015, Radio Spectrum Management, Ministry of Business, Innovation and Employment, New Zealand Government, http://www.rsm.govt.nz/.

[2] J. D. Parsons, *The mobile radio propagation channel*, 2nd ed. Wiley, 2000.

[3] T. T. Street, F. W. Williams, and B. R. Choquette, "The effects of a fire on radio wave transmissions." United States Naval Research Laboratory, Tech. Rep., 1998.

[4] J. Boan, "FDTD for tropospheric propagation with strong cold plasma effects," in *Proc. IEEE APS/URSI Int. Symp.*, 2006, pp. 3905–3908.

[5] K. Mphale and M. Heron, "Microwave measurement of electron density and collision frequency of a pine fire," *Journal of Physics D: Applied Physics*, vol. 40, no. 9, pp. 2818–2825, 2007.

[6] C. Coleman and J. Boan, "A Kirchhoff integral approach to radio wave propagation in fire," in *Proc. IEEE APS/URSI Int. Symp.*, 2007, pp. 3752–3755.

[7] J. Boan, "Radio experiments with fire," *IEEE Antennas Wireless Propag. Lett.*, vol. 6, pp. 411–414, 2007.

[8] J. A. Boan, "Radio propagation in fire environments," Ph.D. dissertation, University of Adelaide, Adelaide, Australia, 2009.

[9] A. C. M. Austin, M. J. Neve, and G. B. Rowe, "Modeling propagation in multifloor buildings using the FDTD method," *IEEE Trans. Antennas Propag.*, vol. 59, no. 11, pp. 4239–4246, 2011.

[10] J. Schneider and F. W. Hofmann, "Absorption and dispersion of microwaves in flames," *Physical Review*, vol. 116, no. 2, pp. 244–249, 1959.

[11] A. Taflove and S. C. Hagness, *Computational Electrodynamics: The Finite-Difference Time-Domain Method*, 3rd ed. Boston: Artech House, 2005.

[12] R. A. Valenzuela, O. Landron, and D. Jacobs, "Estimating local mean signal strength of indoor multipath propagation," *IEEE Trans. Veh. Technol.*, vol. 46, no. 1, pp. 203–212, 1997.

[13] J.-M. Jin, *Theory and Computation of Electromagnetic Fields*. Hoboken, NJ: John Wiley & Sons, 2010.

[14] R. J. Vidmar, "On the use of atmospheric pressure plasmas as electromagnetic reflectors and absorbers," *IEEE Trans. Plasma Sci.*, vol. 18, no. 4, pp. 733–741, 1990.

[15] A. C. M. Austin, N. Sood, J. Siu, and C. D. Sarris, "Application of polynomial chaos to quantify uncertainty in deterministic channel models," *IEEE Trans. Antennas Propag.*, vol. 61, no. 11, pp. 5754–5761, Nov. 2013.

[16] D. Xiu, "Efficient collocational approach for parametric uncertainty analysis," *Commun. Comput. Phys.*, vol. 2, no. 2, pp. 293–309, 2007.